# DOES THE POLEWARD MIGRATION RATE OF THE MAGNETIC FIELDS DEPEND ON THE STRENGTH OF THE SOLAR CYCLE?

V. I. MAKAROV[1], A. G. TLATOV[1] and K. R. SIVARAMAN[2]
[1]*Pulkovo Observatory, 196140, St.Petersburg, Russia*
[2]*Indian Institute of Astrophysics, Bangalore, 560 034, India*

(Received 25 July 2000; accepted 13 April 2001)

**Abstract.** We present the pattern of the polar magnetic reversal for cycle 23 derived from H$\alpha$ synoptic charts and have also included the reversals of the earlier cycles 18–22 for comparison. At the beginning of a new cycle (i.e., soon after the polar reversal) the zonal boundaries of unipolar magnetic regions of opposite polarities (seen as filament bands on the synoptic charts) appear close to and on either side of the equator continuing through the years of minimum indicating the onset of the cancellation of flux at these low latitudes. The cycle thus starts with cancellation of flux close to the equator and ends with the polar reversal or flux cancellation near the poles. The filament bands just below the polemost ones migrate and reach latitudes 35°–45° by the time of polar reversal and become the polemost, once the polar reversal has taken place. During the years of minimum that follow, these filament bands remain more or less stagnant at the latitudes 35°–45° except for occasional slow migration towards the equator. The migration to the poles starts at a low speed of 3 m s$^{-1}$ only when the spot activity has risen to a significant level and then it accelerates to 30 m s$^{-1}$ at the peak of the activity. It takes 3–4 years for the polemost bands to reach the poles moving at these high speeds. We quantify this possible cause and effect phenomenon by introducing the concept of the 'strength of the solar cycle' and represent this by either of a set of three parameters. We show that the velocity of poleward migration is a linear function of the 'strength of the solar cycle'.

## 1. Introduction

One of the puzzling features of solar activity is the way the polar magnetic fields cancel and reversals take place. It is commonly believed that the magnetic activity on the Sun is generated by the dynamo operating in a thin layer at the base of the convection zone (Parker, 1955, 1994; Choudhuri, 1990). At the solar surface the magnetic flux emerges in the form of bipolar regions which are believed to arise from a deep seated toroidal field $B_\phi$. Most active regions follow Hale's law of polarity and the toroidal field has a well-defined east-west orientation. The toroidal field is believed to be generated by the action of differential rotation on poloidal field $B_p$. Dynamic processes responsible for the cycle reversal of the poloidal and toroidal fields are not fully understood. Babcock explained that the magnetic flux from decaying active regions diffuses and eventually forms the large-scale background field. Leighton (1964) proposed that the $f$-polarity fields from the decay of active regions move poleward by a random walk process and cause the polar reversals. It is also recognised that the meridional flows play an important role in

*Solar Physics* **202:** 11–26, 2001.

transporting the field towards the poles ultimately reversing the poloidal field of the solar dynamo (Howard and LaBonte, 1980, 1981; Wang, Nash, and Sheeley, 1989). According to Krause and Rädler (1980) the regeneration of the poloidal field is attributed to the effects of small-scale turbulent flows with a preferred sense of kinetic helicity.

An interesting feature soon after the polar field reversal is the high-latitude solar activity that manifests in the form of polar faculae. The recognition that the polar faculae are an important component of the global cycle is gaining strength as more and more observations on these structures accrue (Makarov and Sivaraman, 1990; Makarov and Makarova, 1996; Erofeev and Erofeeva, 2000). They possess kilogauss fields (Homann, Kneer, and Makarov, 1998). The polar faculae have been identified in the broad band granulation frames of the Soviet Stratoscope flights (spatial resolution $\approx 0.24$ arc sec) and are seen to be made up of a conglomeration of a few structures in the size range of 200–400 km (Makarov *et al.*, 1999). In the high-resolution Ca II–K line scans, the polar faculae are seen as small emission features at the boundaries of the network cells. According to Schrijver *et al.* (1997), the source of flux for the quiet-Sun network component is the ephemeral active regions and that the source flux originates in the convection zone and is not the recycled flux nor the flux transported from the active regions in the lower latitudes. It follows that the source flux for the polar faculae (seen as knots of emission at the network boundaries) is the flux brought out by the ephemeral active regions.

Another aspect pertains to the filament bands and their poleward migration. The unipolar regions identifiable on the magnetograms represent the large-scale magnetic fields on the surface of the Sun. On the H$\alpha$ synoptic charts, the filaments represent the neutral lines that divide the unipolar magnetic regions of opposite polarities. Babcock and Babcock (1955) and Babcock (1959) were the first to map the surface fields on a systematic basis and demonstrate that a magnetic field reversal at the poles took place in the middle of the solar cycle 19 (1955–1965). The subsequent reversals were monitored by Howard (1974). Makarov and Sivaraman (1983) demonstrated that the evolution and migration of the unipolar regions can be studied by monitoring the migration of the neutral lines on the synoptic charts. The mean latitude of a filament band is measured over every 20 deg longitude interval and the average of all such mean latitudes over one rotation provides one data point of the migration trajectory curve on the latitude–time plot. Following this procedure for several rotations, the poleward migration of filaments and finally the polar reversal can be fully mapped. They also demonstrated the excellent agreement between the polar reversals pattern obtained from the filament bands and those from the magnetograms. Following this, they worked out the epochs of polar field reversals over a period of nearly 12 solar cycles (1870–1999) (Figure 1 of Makarov and Sivaraman, 1989a for the years 1870–1980 and extended to 1999 in Figure 1 of this paper). This uncovered an interesting feature that in the even cycles (Nos. 12, 14, 16, 18 and 20, cycle 19 is an exception) there were three fold reversals either in the northern or southern hemisphere. The polar reversals

do not take place at the same time at both the poles and consequently the Sun exhibited the same polarity at both the poles for brief periods of time (see Figure 1 of Makarov and Sivaraman, 1989a). In this paper we describe the zonal structures of unipolar regions and the poleward migration of filament bands in cycle 23. We introduce a new concept namely 'the strength of the solar cycle' and represent this quantitatively by either of the three parameters. We show that the speed of the poleward migration of the filament bands is linearly related to these parameters. We also discuss some questions regarding the role of the meridional circulation in transporting the fields towards the poles.

## 2. Observational Data

Observational data on polar migration of magnetic fields were obtained on the H$\alpha$ synoptic charts that reflect the distribution of polarity of a magnetic field (McIntosh, 1979; Makarov and Fatianov, 1980; Makarov and Sivaraman, 1989a, b, 1990). From the H$\alpha$ synoptic charts of the Kislovodsk solar station for the period 1975–2000, we constructed the latitude-time maps that show the episodic migration trajectory of the filament bands following the procedure described by Makarov, Fatianov, and Sivaraman, 1983). By combining this with similar latitude-time maps for the earlier periods (Figure 1 of Makarov and Sivaraman, 1989a, for the years 1870–1980) we constructed the latitude positions of all filament bands on the Sun for the period 1880–2000 (not shown here). Wolf numbers, number of sunspot groups and sunspot areas for this period were taken from Jones (1955), Hoyt and Schatten (1998), Makarov and Makarova (1996), *Solnechnye Dannye* (1996–1999).

## 3. Results and Discussion

In Figure 1 we show the position of the mean latitude of the filament bands in solar cycles 18–23 (1950–2000). At the minimum of activity in 1995, the zonal boundaries of the polemost filament bands designated by $\Theta_{\mathrm{N},2m}$ and $\Theta_{\mathrm{S},2m}$ in the N and S hemispheres and shown by filled circles in Figure 1 were located at latitudes $\Theta_{\mathrm{N},2m} = 36^\circ$ and $\Theta_{\mathrm{S},2m} = 39^\circ$. The next lower filament bands designated by $\Theta_{\mathrm{N},1m}$ and $\Theta_{\mathrm{S},1m}$ in the N and S hemispheres were located at latitudes $\Theta_{\mathrm{N},1m} = 18^\circ$ and $\Theta_{\mathrm{S},1m} = 22^\circ$ (shown by open circles in Figure 1).

During the years of minimum spot activity, the polar faculae were present at latitudes $\approx 50^\circ$ and higher in the N and S hemispheres and the filament bands remained more or less steady at the latitudes they have already reached but for a slow progression equatorwards for nearly 4 years (1992–1996). This equatorward movement is less obvious in other cycles. Although the polar reversal took place in 1991 the migration towards the poles started only by 1996 (with a speed of

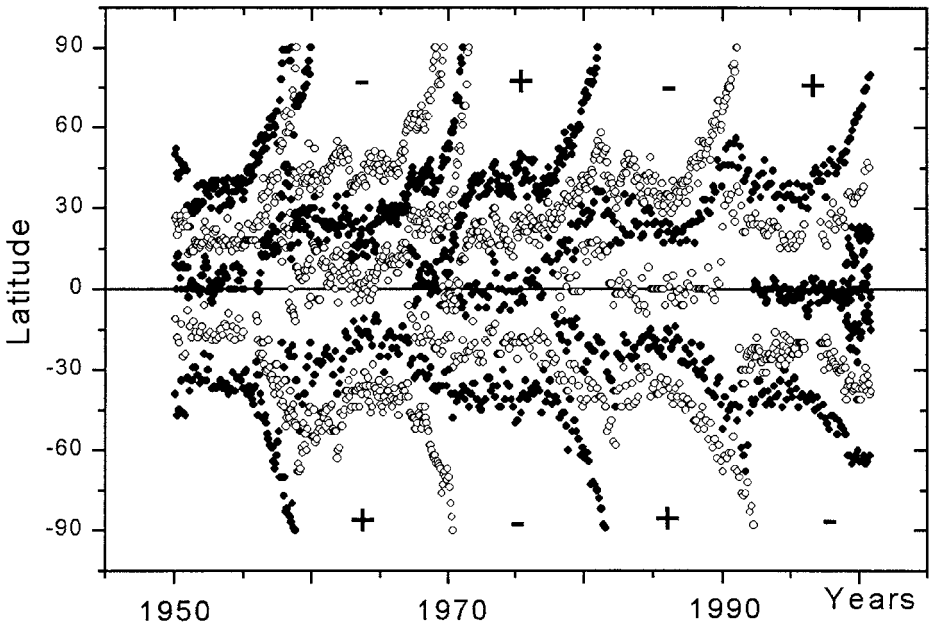


*Figure 1.* Migration trajectories of magnetic neutral lines (*alias* filament bands) of the large-scale magnetic fields derived from H$\alpha$ synoptic charts in the N and S hemispheres for the period 1950–2000. In the north, *filled circles* represent the neutral line trajectory with the opposite polarities on either of its sides in the order (+/−) and *open circles* represent the trajectory of the neutral line with polarities on either of its sides in the order (−/+). In the south it is in the reverse order. Note the zonal structure of the global magnetic field on the surface.

$V_{pw} \approx$ 3 m s$^{-1}$) when the sunspot activity picked up at the middle latitudes. By 2000.4 (rotation No. 1961) these zonal boundaries migrated polewards in the northern hemisphere to locations $\Theta_{\mathrm{N},2m} = 70°$ and $\Theta_{\mathrm{N},1m} = 40°$ and to locations in the southern hemisphere $\Theta_{\mathrm{S},2m} = 68°$ and $\Theta_{\mathrm{S},1m} = 43°$.

In addition, two more zonal boundaries formed at latitudes $\Theta_{\mathrm{N},0m} = 20°$ and $\Theta_{\mathrm{S},0m} = -19°$. The dominant mode in the latitude zonal structure is seen to be $l = 5$ ($l$ is the number of neutral lines present on the surface with $m = 0$) as in the years 1956–1958 and 1972–1977. Higher modes $l = 7$ are also seen occasionally as in the years 1968–1970 (see also Figure 1 of Makarov, 1984) and in the current cycle. One interesting feature in Figure 1 is the formation of a new low-latitude zone at the beginning of each cycle close to the equator and this is obvious in a high-resolution plot (Figure 1 of Makarov, 1984). This would imply that the magnetic field reversal takes place close to the equator at the beginning of the cycle continuing through the years of minimum and this is an indication of the flux cancellation by the fragmented flux from spots very close to the equator which are the last vestiges of the cycle. Another feature seen in Figure 1 of this study (also Figure 1 of Makarov, 1984) is that when the sunspot activity reaches its peak, the polemost filament bands at the latitudes $\approx$ (45°–50°) suddenly accelerate with

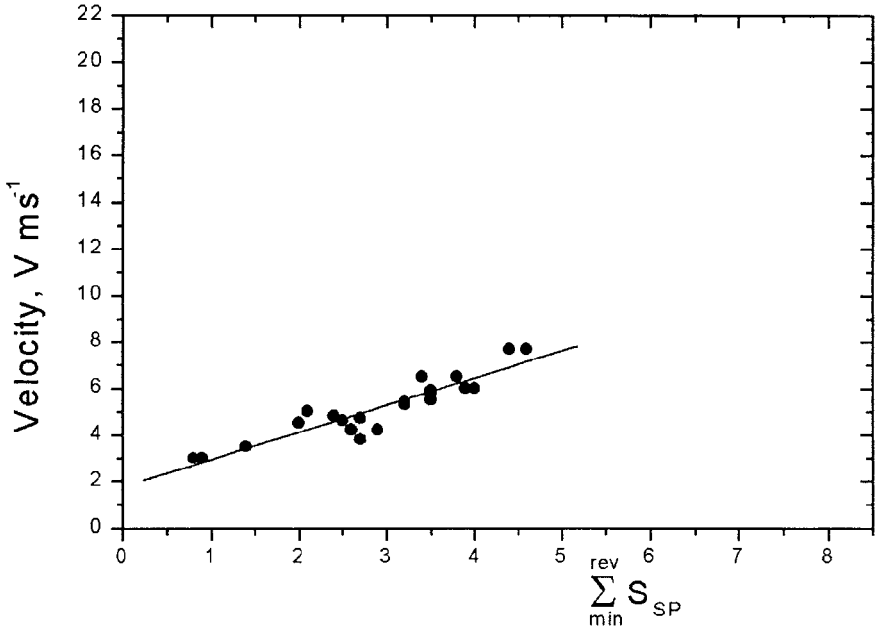


*Figure 2.* Plot of $\Sigma_{min}^{rev} S_{sp}$ vs. velocity $V_{pw}$ of polemost filament. $\Sigma_{min}^{rev} S_{sp}$ values are from Table I and velocity values are from Table III. *Filled circles* represent single-fold reversals and the first wave of the 3-fold reversals. The N and S are not distinguished.

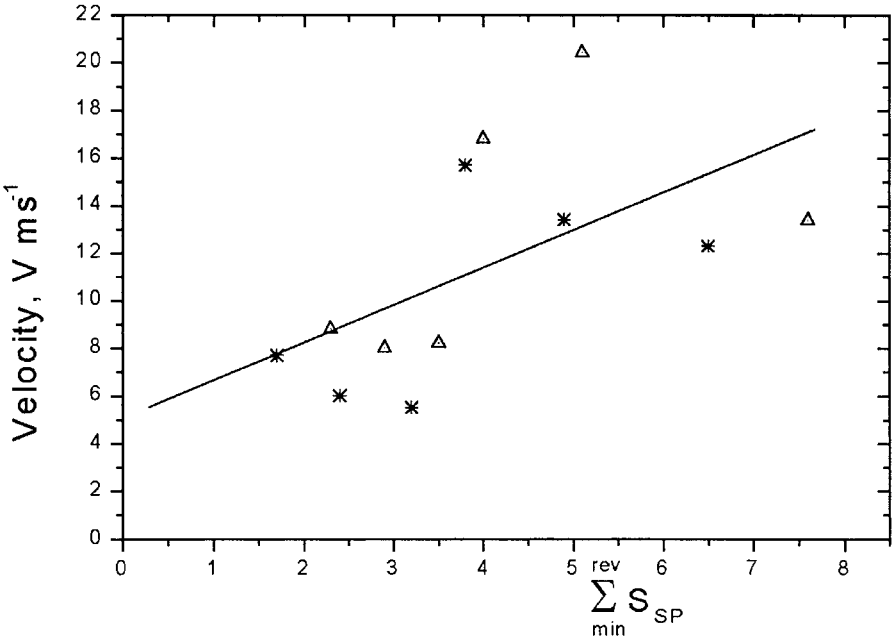


*Figure 3.* Plot of $\Sigma_{min}^{rev} S_{sp}$ vs. velocity $V_{pw}$ of polemost filament. $\Sigma_{min}^{rev} S_{sp}$ values are from Table I and velocity values are from Table III. *Stars* represent the second and *open triangles* represent the third waves of the 3-fold reversals. The N and S are not distinguished.

almost a ten-fold increase in speed in their poleward migration (accelerates from 3 m $s^{-1}$ up to about 30 $=$ m $s^{-1}$) and reach the poles in about 3 years causing the polar field reversal.

The estimated speed of 30 m $s^{-1}$ represents the average rate of migration of the filament bands for the drift time from 40° latitude all the way to the poles. We have done the averaging as both the starting and ending spatial and temporal points of the poleward journey can be estimated with confidence. Here we have assumed that, the epoch of the disappearance of the polar prominences represents the completion of the polar reversal which in turn marks the end of the poleward migration of the filament bands. This averaging is a good trade-off considering the possible errors that might arise while attempting to measure the migration rate particularly at high latitudes due to the curved geometry.

This rapid migration phase is the 'rush to the poles' by the neutral lines that form a continuous chain of filaments encircling both the hemispheres near the N and S poles (also known as the polar crown filaments) described by earlier workers like the D'Azambujas (1948) and Ananthakrishnan and Nayar (1953) who estimated the speed of migration to be 0.9 deg per rotation between latitudes 40–70 deg. Further the D'Azambujas (1948), using the long-lived H$\alpha$ dark markings, noticed that the rate of poleward drift in the high-latitude zone was twice as fast in the ascending phase of the sunspot cycle than in the descending phase and they interpreted this as an evidence for the existence of a meridional circulation. In recent times McIntosh (1992) has studied the migration in detail for cycles 21 and 22 using the H$\alpha$ synoptic maps. The filament bands below the polemost ones also commence their poleward journey synchronously and proceed almost at the same high speed as the polemost filament bands. But if the sunspot activity subsides by the time they reach the latitudes $\pm$45°, then these filament bands abruptly stop their poleward journey and either remain at the latitude they already are or at times tend to move towards the equator at very low speeds for a short period and stay at that latitude. This is what happens in a single-fold reversal.

Whereas in a three-fold reversal, the filament bands just below the polemost ones also reach latitudes $\pm$(45°–50°) while the sunspot activity is still in progress and so they proceed poleward with the same high speed as the polemost ones and reach the poles, and this is followed by the third filament band, too, causing the final reversal of the three-fold reversal process. The three-fold reversal seems to be generally a characteristic of cycles with high and persistant sunspot activity, if not it ends up in a single-fold reversal. These situations raise questions about the role of the meridional motions in transporting the fields towards the poles. Why does the meridional circulation become effective only with the rapid rise in solar activity and not during the years of minimum? None of the filament bands show any sign of poleward journey during the years of solar minimum. As soon as the sunspot activity picks up, the filament starts the poleward journey with a speed of $V_{pw} \approx$ 3 m $s^{-1}$ and when the activity reaches high levels, it accelerates to $V_{pw} \approx$ 30 m $s^{-1}$. This may mean that either the meridional flows are weaker

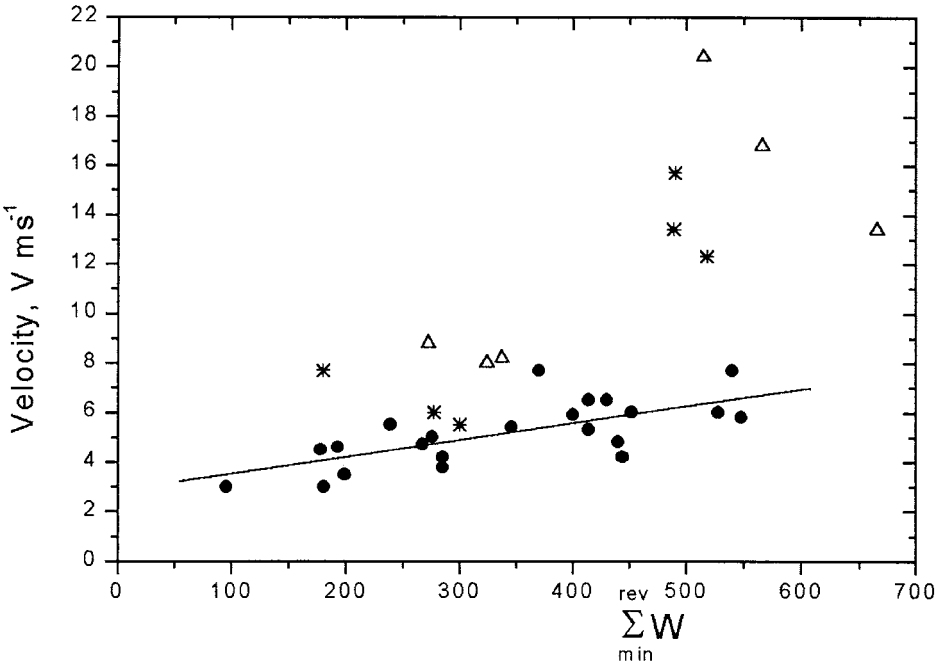


*Figure 4.* Plot of $\Sigma^{rev}_{min} W$ vs. velocity of the polemost filament. $\Sigma^{rev}_{min} W$ values are from Table II and velocity from Table III. *Filled circles* represent single-fold reversals and the first wave of the 3-fold reversals, *stars* represent the second and *open triangles* represent the third waves of the 3-fold reversals. $\Sigma^{rev}_{min} W$-summation of the annual means (from the monthly means) of the Wolf numbers, but over the entire visible hemisphere starting from the lowest value of the annual mean in $W$ in the minimum phase all the way to the year of the polarity reversal.

during the years of minimum or there is no significant flux in the sunspot belt (due to the paucity of sunspots during the years of deep minimum) to be transported although the meridional flows are present all the time with no significant cycle related changes. Although the latter possibility would seem more realistic and consistent with the modest dynamical concepts of flows on the solar surface we cannot rule out the possibility of a cycle dependence which according to Snodgrass and Dailey (1996) is rather complex but does not disagree with our results. The measurements of the Sun's meridional circulation show that it is slow and is of the order of 10 m s$^{-1}$. The measurements by Duvall (1979), Topka *et al.* (1982), Ulrich *et al.* (1988), Howard (1991), Komm, Howard, and Harvey (1993) use different diagnostics like Doppler signals, feature tracking, etc., and so may not be directly comparable as these motions pertain to different levels in the atmosphere or in the interior. Also, each of these measurements pertains to periods small compared to the length of the solar cycle and to different phases of different cycles. Thus the difficulty of retrieving the meridional flow signals from other systematic flow signals (which themselves are not time invariant) coupled with the possibility of a solar cycle dependence has produced a wide range of quoted flow speeds and

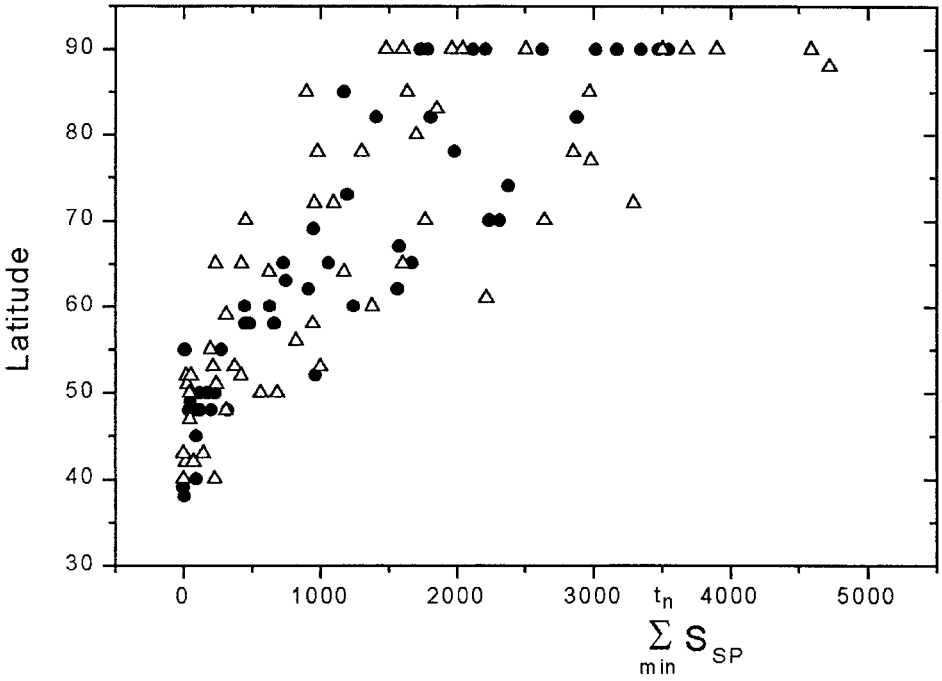


*Figure 5.* Plot of $\Sigma_{\min}^{\mathrm{rev}} S_{sp}$ vs. latitude of the polemost filament (see text for details). *Filled circles* represent $\Sigma_{\min}^{t_n} S_{sp}$ (in $10^{-3}$ of the visible hemisphere) in the N-hemisphere and *triangles* in the S-hemisphere.

its variations with latitude. Recently Hathaway (1996) has detected poleward flow with typical speeds of 20 m s$^{-1}$ and that there are short episodes with much stronger flows in the range of 30 m s$^{-1}$ to 80 m s$^{-1}$ using the GONG data for the period mid-1992 to early 1995. Although the period of this study is too short to point to any possible long-term solar-cycle-related changes, the evidence that the flow speeds are episodical and can vary over a wide range of values seems certain. However, a final confirmation of this should be forthcoming soon either from the MDI data on SOHO (Meunier, 1999) or from the helioseismic data.

On the other hand, in our study, if there are no magnetic tracers available to be transported we would not perceive any motion although it might be present all the time. We have seen that only when the spot activity has picked up, the polemost filaments cross the $\pm 45°$ latitudes with accelerated speeds and cause the reversal. While, if the sunspot activity has subsided by the time the filament band just below the polemost one reaches the ($45° - 50°$) latitude position, then it does not proceed further but hovers around the 45° latitude belt until the sunspot activity of the next cycle builds up. This indicates that the remnant flux from decaying active regions that still remain on the surface (even after cancellation, submergence, etc.) does not constitute a body of flux sufficient to effect further cancellation and hence the neutral line does not shift towards the poles. This neutral line (now the polemost

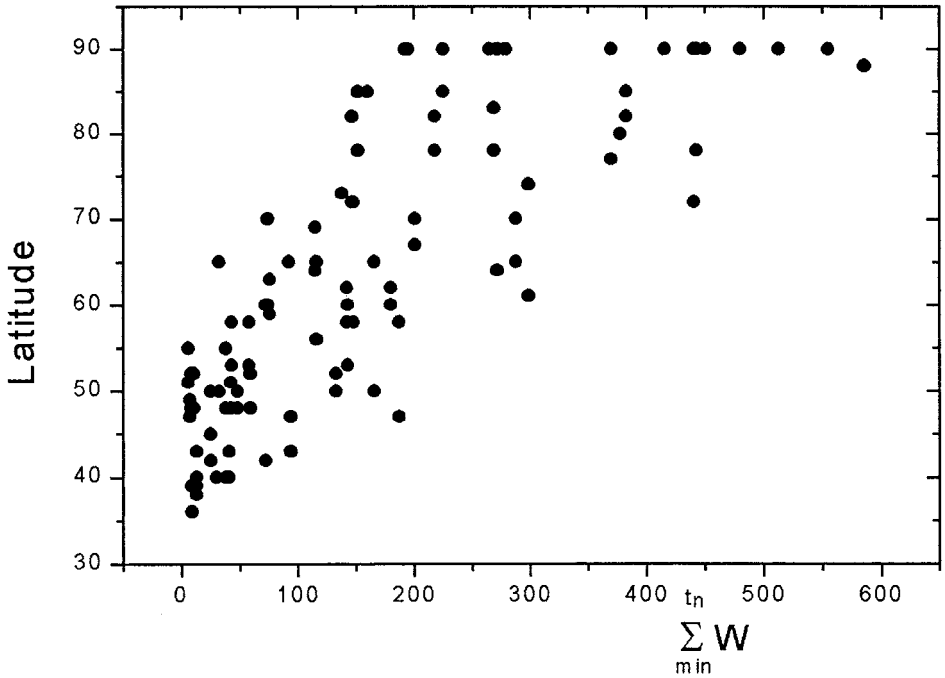


*Figure 6.* Plot of $\Sigma_{\min}^{t_n} W$ vs. latitude of the polemost filament bands. $\Sigma_{\min}^{rev} W$-summation of the annual means (from the monthly means) of the Wolf numbers, but over the entire visible hemisphere (see text for details).

one) seems to wait for the activity of the next cycle to build up to start its poleward journey. Also the $\pm(45°-50°)$ belt seems to act like a boundary where the decision whether the filament band will proceed poleward or stay stagnant takes place. Thus the poleward migration of the neutral lines seems to depend very sensitively on the sunspot activity (Makarov and Callebaut, 1999). Although at this stage we do not have evidence even to speculate on the dynamical implications, if at all, of this latitude belt $(45°-50°)$ we would use this ocassion to bring to the notice of the reader two phenomena possibly related, where this latitude belt may seem dynamically important. The first one is the surface rotation vs. latitude profile that Stenflo (1989) derived from the Kitt Peak magnetograms. He finds that until 40° latitude the rotation matches well with the rotation law of Snodgrass (1983) but beyond 40° it becomes more rigid. This rigid rotation reverses to a polar spin up at $\approx$ 50° latitude. The second one is the discovery of the inversion of the radial gradient of the angular velocity that occurs at this latitude belt in the subsurface rotational shearing layer from helioseismic studies (Schou *et al.*, 1998).

The latitude–time plot of the migration of the filament bands for cycle 19 (Figure 2 of Makarov and Sivaraman, 1989b) shows qualitatively the unmistakable dependence of the rate of poleward migration on the level of sunspot activity. The

TABLE I

Values of $\Sigma^{\rm rev}_{\rm min} S_{sp}$: these are the sums of the annual means of sunspot areas $S_p$ for the N and S hemisphere (in $10^{-3}$ of the area the visible hemisphere) starting from the lowest value of $S_p$ of the minimum years all the way to the year of polar reversal for cycles 12–22 (1880–1990). In either hemisphere the single values of $\Sigma^{\rm rev}_{\rm min} S_{sp}$ represent the single-fold reversals and the blocks of three values represent the three-fold reversals.

| Hemisphere | Cycles | | | | | | | | | | | |
|---|---|---|---|---|---|---|---|---|---|---|---|---|
| | 12 | 13 | 14 | 15 | 16 | 17 | 18 | 19 | 20 | 21 | 22 | 23 |
| N | 0.8 | 2.7 | 2.0 | 2.7 | 2.5 | 4.0 | 3.2 | 4.4 | 3.2 | 3.4 | 3.5 | – |
| N | – | – | – | – | 3.2 | – | 3.8 | 6.5 | 4.9 | – | – | – |
| N | – | – | – | – | 3.5 | – | 4.0 | 7.6 | 5.1 | – | – | – |
| S | 1.4 | 2.9 | 0.9 | 2.1 | 3.5 | 2.6 | 3.8 | 4.6 | 2.4 | 3.5 | 3.9 | – |
| S | 2.4 | – | 1.7 | – | – | – | – | – | – | – | – | – |
| S | 2.9 | – | 2.3 | – | – | – | – | – | – | – | – | – |

sudden acceleration that the filament bands experience with the rise in the level of sunspot activity can also be seen in this Figure.

To quantify this dependence we define three variables $S_{sp}$, $W$, and $R_g$ for each cycle where $\Sigma^{\rm rev}_{\rm min} S_{sp}$-summation of all the annual means of sunspot areas $S_{sp}$ of the cycle (for the N and S hemispheres separately) starting from the lowest value of the annual mean in $S_{sp}$ in the minimum phase all the way to the year of the polarity reversal, $\Sigma^{\rm rev}_{\rm min} W$-summation of the annual means (from the monthly means) of the Wolf numbers, but over the entire visible hemisphere starting from the lowest value of the annual mean in $W$ in the minimum phase all the way to the year of the polarity reversal. We have classified them to the N and S hemispheres according to the epoch of when polar magnetic field reversals occurred in these two hemispheres, $\Sigma^{\rm rev}_{\rm min} R_g$-summation of the number of sunspot groups as done for $\Sigma^{\rm rev}_{\rm min} W$, but over the entire visible hemisphere. Each of these parameters according to us represents the 'strength of the solar cycle' although they are not independent of each other.

In Table I we present the values of $\Sigma^{\rm rev}_{\rm min} S_{sp}$ (in units of $10^{-3}$ of the area of the visible hemisphere) for the N and S hemispheres. In the north hemisphere there is only one value of $\Sigma^{\rm rev}_{\rm min} S_{sp}$ in cycles 12 to 15, 17, 21, and 22 and these correspond to single polar reversals in these cycles while the three values in cycles 16, 18, 19, and 20 pertain to the three successive waves of the three-fold reversals. Similarly in the south hemisphere the single values in cycles 13 and 15 to 22 correspond to the single reversals in these cycles and the three values in cycles 12 and 14 correspond to the three-fold reversals.

Table II contains the values of $\Sigma^{\rm rev}_{\rm min} W$ for the cycles 12–22. The values of $W$ always pertain to the entire visible hemisphere, but we have classified them (in Table II) to the N and S hemispheres according to the epoch of when polar

TABLE II

Values of $\Sigma_{\min}^{\text{rev}} W$ – these are the sums of the annual means (from the monthly means) of the Wolf numbers, but over the entire visible hemisphere starting from the lowest value of the annual mean in W in the minimum phase all the way to the year of the polarity reversal for cycles 12–22. The values $\Sigma_{\min}^{\text{rev}} W$ for the entire visible hemisphere have been classified to the N and S hemispheres according to the epoch of when polar magnetic field reversals occurred in the two hemispheres. The single values represent the single-fold reversals and the blocks of three values represent the three-fold reversals.

| Hemisphere | Cycles | | | | | | | | | | | |
|---|---|---|---|---|---|---|---|---|---|---|---|---|
| | 12 | 13 | 14 | 15 | 16 | 17 | 18 | 19 | 20 | 21 | 22 | 23 |
| N | 181 | 285 | 178 | 267 | 193 | 452 | 414 | 370 | 346 | 430 | 400 | – |
| N | – | – | – | – | 300 | – | 490 | 518 | 489 | – | – | – |
| N | – | – | – | – | 337 | – | 566 | 666 | 515 | – | – | – |
| S | 199 | 285 | 96 | 276 | 239 | 444 | 414 | 540 | 440 | 548 | 528 | – |
| S | 277 | – | 180 | – | – | – | – | – | – | – | – | – |
| S | 324 | – | 272 | – | – | – | – | – | – | – | – | – |

TABLE III

The migration velocity (in m $s^{-1}$) of the polemost filament band (zonal boundary of the magnetic field) from the H$\alpha$ synoptic charts for cycles 12–22 (1880–1990). The velocity values are the means over the same period as $\Sigma_{\min}^{\text{rev}} S_{sp}$ are summed (starting from the year of the lowest $S_p$ all the way to the year of polar reversal.

| Hemisphere | Cycles | | | | | | | | | | | |
|---|---|---|---|---|---|---|---|---|---|---|---|---|
| | 12 | 13 | 14 | 15 | 16 | 17 | 18 | 19 | 20 | 21 | 22 | 23 |
| N | 3.0 | 3.8 | 4.5 | 4.7 | 4.6 | 6.0 | 5.3 | 7.7 | 5.4 | 6.5 | 5.9 | – |
| N | – | – | – | – | 5.5 | – | 15.7 | 12.3 | 13.4 | – | – | – |
| N | – | – | – | – | 8.2 | – | 16.8 | 13.4 | 20.4 | – | – | – |
| S | 3.5 | 4.2 | 3.0 | 5.0 | 5.5 | 4.2 | 6.5 | 7.7 | 4.8 | 5.8 | 6.0 | – |
| S | 6.0 | – | 7.7 | – | – | – | – | – | – | – | – | – |
| S | 8.0 | – | 8.8 | – | – | – | – | – | – | – | – | – |

magnetic field reversals occurred in these two hemispheres to enable a comparison with $\Sigma^{\rm rev}_{\rm min} S_{sp}$-velocity plot.

In Table III we present the values of the migration velocity ($V_{pw}$ in m s$^{-1}$) of the filament bands for cycle 12–22. This velocity is the average speed over the period starting from the lowest value of the annual mean in $S_{sp}$ in the minimum phase all the way to the year of the polarity reversal. We have classified them to the N and S hemispheres according to the epoch of when polar magnetic field reversals occurred in these two hemispheres.

In addition to the three parameters we have introduced ($\Sigma^{\rm rev}_{\rm min} S_{sp}$, $\Sigma^{\rm rev}_{\rm min} W$, and $\Sigma^{\rm rev}_{\rm min} R_g$) it should be possible to define a few more, like the average magnetic flux that can be derived from full-disk magnetograms. But these data cover much shorter periods (2 or 3 cycles) than we have included in our study. We could not have estimated the magnitude of this average flux from the H$\alpha$ synoptic charts as they show only the distribution of polarities.

In Figure 2 we have plotted the values of $\Sigma^{\rm rev}_{\rm min} S_{sp}$ (from Table I) against the corresponding values of velocity $V_{pw}$ for single-fold reversals and the first wave of the 3-fold reversals (from Table III). The linear fit to the data points of the single reversal and the first reversal of the three-fold reversal are given by the equation

$$V_{pw}\ (\mathrm{m\ s^{-1}}) \approx (1.8 \pm 0.4) + (1.2 \pm 0.1)\ \Sigma^{\rm rev}_{\rm min} S_{sp}. \tag{1}$$

We have 22 data points for the single reversal and so a least square fit is possible with confidence, whereas there are only 6 data points each for the second and third reversals. Nevertheless we show a least-squares fit with the small number of data points. Figure 3 shows the data points of the second and third reversals of cycles 12, 14, 18, 19, 20. One can see that this activity of the magnetic field belongs to a different regime,

$$V_{pw}\ (\mathrm{m\ s^{-1}}) \approx (5.3 \pm 3.0) + (1.5 \pm 0.7)\ \Sigma^{\rm rev}_{\rm min} S_{sp}. \tag{2}$$

Figure 4 shows the plot of $\Sigma^{\rm rev}_{\rm min} W$ vs. velocity $V_{pw}$ (from Tables II and III). All the data points of the single-fold reversal as well as of the first reversal of the three-fold reversals show a clear linear trend,

$$V_{pw}\ (\mathrm{m\ s^{-1}}) \approx (2.7 \pm 0.6) + (0.007 \pm 0.002)\ \Sigma^{\rm rev}_{\rm min} W. \tag{3}$$

The plot of $\Sigma^{\rm rev}_{\rm min} R_g$ vs. velocity $V_{pw}$ (not shown here) is identical to the plots in Figure 4. The linear fits to the data points of the single reversal and the first reversal of the three-fold reversal are similar to $\Sigma^{\rm rev}_{\rm min} W$,

$$V_{pw}\ (\mathrm{m\ s^{-1}}) \approx (2.8 \pm 0.6) + (0.007 \pm 0.002)\ \Sigma^{\rm rev}_{\rm min} R_g. \tag{4}$$

It can be seen that the rate of polar drift at the times of low sunspot activity is only about 2 m s$^{-1}$ and if the filament bands were to migrate all the time at this low speed, it would take almost 20 years (which is greater than the duration of one cycle) even for the polemost filament bands to reach the respective poles.

It is tempting to speculate that such low poleward velocities might have been a characteristic of the Maunder minimum years.

If $S_{sp}$ or $W$ has a declining trend in the first half of the cycle, then the zonal boundaries cease to move polewards but they fold back (equatorward) to latitudes about 40° (Makarov and Sivaraman, 1989b). Thus an increase in the spot activity above a certain threshold (not possible to define from this study ) in the first half of the cycle seems to be a condition necessary for the poleward velocity to reach a high value sufficient to transport the fields polewards and effect the polar reversal in the corresponding hemisphere within the duration of the cycle. This along with the trend in the $\Sigma_{\min}^{\text{rev}} S_{sp}$ vs. velocity $V_{pw}$ and $\Sigma_{\min}^{\text{rev}} W$ vs. velocity $V_{pw}$ relations would imply that a part of the magnetic flux from decayed active regions in the sunspot belt (from sunspots that lived and died long ago) still wanders around and is transported towards the poles.

It might be too naive to imagine that the Sun would transport to the poles only just the right amount of flux required for cancellation. Therefore it may not be unreasonable to assume that certain amount of the equatorial flux transported would be left over at the high latitudes after the cancellation and this would add to the existing large-scale fields from other sources. We are attempting to estimate the dynamic flux on the solar surface from different sources to understand these situations and this would be the subject of discussion of a later paper.

It might be interesting to recall that the transport of surface magnetic fields towards the poles has been modeled by Sheeley and coworkers (1992), invoking differential rotation, random walk diffusion, and a time invarying meridional flow. Recently, Van Ballegooijen, Cartledge, and Priest (1998) have a model that better fits with observations. Although these models reproduce the poleward migrations at the appropriate phases of the solar cycle in a gross sense, they fail to reproduce the pattern of behaviour of the neutral lines seen in the H$\alpha$ synoptic charts in matters of details, like the long periods when the polemost filaments stay at the 50° latitude zones without any visible migration either polewards or equatorwards or the episodic surges in the poleward drift at high speeds or the non-simultaneous polar reversals that occur at the N and S poles.

Another interesting aspect brought out in this study is that the 'strength of the solar cycle' is a deciding factor also of the maximum latitudes to which the polemost filament bands can reach during a solar cycle. To illustrate this point, we have related the running sums of the annual means of the sunspot areas $\Sigma_{\min}^{t_n} S_{sp}$ and of the Wolf sunspot numbers $\Sigma_{\min}^{t_n} W$ with latitudes of the polemost filament bands. We obtain these quantities in the following way for each cycle.

$\Sigma_{\min}^{t_1} S_{sp}$ is just the lowest annual mean value of the sunspot area (separately for the N and S hemispheres) in the minimum years of any cycle. This single annual mean of the first year is the first data point in that cycle. The use of $\Sigma$ for this term is just to maintain uniformity with the remaining terms that follow although no summation is involved in this term.

$\Sigma_{\min}^{t_2} S_{sp}$ is the second data point is the sum of the annual means of $S_{sp}$ of the first and second years, and so on.

$\Sigma_{\min}^{t_r} S_{sp}$ is the last data point is the sum of all the annual means of $S_{sp}$ of the years 1 to r, where r is the year of the polar reversal.

We represent this running series of sums by the symbol $\Sigma_{\min}^{t_n} S_{sp}$ where $t_n$ runs from $t_1$ to $t_r$. Thus for any cycle, we have as many $\Sigma_{\min}^{t_n} S_{sp}$ as there are years from 1 to r. We have done this for every cycle from cycle 12 to 22.

We have obtained in a similar way the running series of sums of the annual means of the Wolf sunspot numbers (for the entire visible hemisphere) and represent them $\Sigma_{\min}^{t_n} W$, where $t_n$ runs from $t_1$ to $t_r$.

The latitudes corresponding to each data point of the running series in a cycle is the latitude of the polemost filament band (averaged over the N and S) in the last month of the last year to which $S_{sp}$ (or W) is summed. In Figures 5 and 6 we have plotted the data points of $\Sigma_{\min}^{t_n} S_{sp}$ vs. latitude and $\Sigma_{\min}^{t_n} W$ vs. latitude from cycles 12 –22. It can be seen that for filament bands to reach the poles $\Sigma_{\min}^{t_n} W$ should at least have a value of $\approx$ 250 and $\Sigma_{\min}^{t_n} S_{sp}$ a value of $\approx 1500$. A value of $\Sigma_{\min}^{t_n} W \approx 250$ corresponds to $W_{\max} \approx 40$. It means that a polar reversal of the magnetic field of the Sun requires minimum activity corresponding to the value of $W_{\max} \approx 40$.

## 4. Conclusion

(1) We have presented the polar magnetic field reversal pattern for cycle 23 derived from the H$\alpha$ synoptic charts (Figure 1). The formation of a new zone close to the equator at the beginning of each cycle implies that magnetic reversal takes place close to the equator at the beginning of the cycle. Thus the flux cancellation near the equator marks the beginning of a solar cycle while the flux cancellation at the poles marks the end of that cycle.

(2) We have established for the first time that the velocity of the poleward migration of the filament bands bears a linear relation with the 'strength of the solar cycle'. We represent this quantity by three parameters. This would imply that part of the flux from the sunspot belt transported to high latitudes would effect the cancellation of the polar fields at the time of the polar reversals and the excess flux would remain there and add to the *in-situ* large-scale fields from other sources at the high latitudes.

(3) The 'strength of the solar cycle' also decides the maximum latitude to which the polemost filaments can reach during the cycle. The value of $\Sigma_{\min}^{t_n} S_{sp}$ has to be at least 1500 or $W_{\max} \approx 40$ for the polemost filaments to reach the poles and complete the reversal process.

## Acknowledgements

We wish to express our thanks to Prof. R. Cowsik, Director, Indian Institute of Astrophysics, for his kind encouragement. Part of the work was carried out during the visit of V. I. Makarov and A. G. Tlatov to the Indian Institute of Astrophysics, Bangalore and Kodaikanal under the Scientific Exchange Programme (ILTP) between the Russian Academy of Sciences and the Indian National Science Academy. This work was supported in part by the Russian Foundation for Basic Research, grants 99-02-16200, 00-02-16355, INTAS 97-1088 and NRA-OSS-08. We are thankful to the referee for providing valuable comments that have helped in improving the clarity of some of the points in the paper.

## References

Ananthakrishnan, R. and Madhavan Nayar, P.: 1953, *Kodaikanal Obs. Bull.* No. 137, 194.
Babcock, H. W. and Babcock, H. D.: 1955, *Astrophys. J.* **121**, 349.
Babcock, H. D.: 1959, *Astrophys. J.* **130**, 364.
Choudhuri, A. R.: 1990, *Astrophys. J.* **355**, 733.
D'Azambuja, L. and D'Azambuja, M.: 1948, *Ann. Obs. Meudon* **6**, VII.
Duvall, T. L., Jr.: 1979, *Solar Phys*. **63**, 3.
Erofeev, D. V. and Erofeeva, A. V.: 2000, *Solar Phys.* **191**, 281.
Hathaway, D. W.: 1996, *Astrophys. J.* **460**, 1027.
Homann, T., Kneer, F., and Makarov, V. I.: 1998, *Solar Phys.* **175**, 81.
Howard, R.: 1974, *Solar Phys.* **38**, 283.
Howard, R.: 1991, *Solar Phys.* **131**, 259.
Howard, R. and LaBonte, B. J.: 1980, *Astrophys. J.* **239**, L33.
Howard, R. and LaBonte, B. J.: 1981, *Solar Phys.* **74**, 31.
Hoyt, D. V. and Schatten, K. H.: 1998, *Solar Phys.* **157**, 340.
Jones, H. S.: 1955, *Sunspot and Geomagnetic Storm Data*, Her Majesty's Stationery Office, London.
Komm, R. W., Howard, R. F., and Harvey, J. W.: 1993, *Solar Phys.* **147**, 207.
Krause, F. and Rädler, K. H.: 1980, *Mean Field Magnetohydrodynamics and Dynamo Theory*, Pergamon Press, Oxford.
Leighton, R. B.: 1964, *Astrophys. J.* **140**, 1547.
Makarov, V. I.: 1984, *Solar Phys.* **93**, 393.
Makarov, V. I. and Fatianov, M. P.: 1980, *Solnechnye Dannye*, No. 10, 96.
Makarov, V. I. and Makarova, V. V.: 1996, *Solar Phys.* **163**, 267.
Makarov, V. I. and Sivaraman, K. R.: 1983, *Solar Phys*. **85**, 227.
Makarov, V. I. and Sivaraman, K. R.: 1989a, *Solar Phys.* **119**, 35.
Makarov, V. I. and Sivaraman, K. R.: 1989b, *Solar Phys.* **123**, 367.
Makarov, V. I. and Sivaraman, K. R.: 1990, in J. O. Stenflo (ed.), Solar Photosphere: Structure, Convection, and Magnetic fields, *IAU Symp.* **138**, 281.
Makarov, V. I., Fatianov, M. P., and Sivaraman, K. R.: 1983, *Solar Phys.* **85**, 215.
Makarov, V. I., Okunev, O. V., Pravdjuk, L. M., and Kneer, F.: 1999, in A. Antalova, H. Balthasar, and A. Kucera (eds.), *Annual Report 1998, Joint Organisation for Solar Observations*, Astronomical Institute, Tatranská Lomnica, p. 151.
Makarov, V. I. and Callebaut, D. K.: 1999, in A. Wilson (ed.), *Proc. 9th European Meeting on Solar Physics, 'Magnetic Field and Solar Processes', Florence, Italy*, p. 117.

McIntosh, P. S.: 1979, *Annotated Atlas of H-alpha Charts*, NOAA, Boulder.
McIntosh, P. S.: 1992, in Karen L. Harvey (ed.), *The Solar Cycle, ASP Conf. Series*, **27**, 14.
Meunier, N.: 1999, *Astrophys. J.* **527**, 967.
Parker, E. N.: 1955, *Astrophys. J.* **121**, 491.
Parker, E. N.: 1994, in M. Schüssler and W. Schmidt (eds.), *Solar Magnetic Fields*, Proc. Int. Conf. Freiburg, Germany, June 29 – July 2, 1993, Cambridge University Press, Cambridge, p. 94.
Schou, J. *et al.*: 1998, *Astrophys. J.* **505**, 390.
Schrijver, C. J., Title, A. M., van Ballegooijen, A. A., Hagenaar, H. J., and Shine, R. A.: 1997, *Astrophys. J.* **487**, 424.
Sheeley, N. R., Jr.: 1992, in Karen L. Harvey (ed.), *The Solar Cycle, ASP Conf. Series* **27**, 1.
Snodgrass, H. B.: 1983, *Astrophys. J.* **270**, 288.
Snodgrass, H. B. and Dailey, S. B.: 1996, *Solar Phys.* **163**, 21.
*Solnechnye Dannye*: 1996–1999, *Soln. Dann.* Nos. 1–12.
Stenflo, J. O.: 1989, *Astron. Astrophys.* **210**, 403.
Topka, K., Moore, R., La Bonte, B. J., and Howard, R. F.: 1982, *Solar Phys.* **79**, 231.
Ulrich, R. K., Boyden, J. E., Webster, L., Snodgrass, H. B., Padilla, S. P., Gilman, P., and Shieber, T.: 1988, *Solar Phys.* **117**, 291.
Van Ballegooijen, A. A., Cartledge, N. P., and Priest, E. R.: 1998, *Astrophys. J.* **501**, 866.
Wang, Y. M., Nash, A. G., and Sheeley, N. R., Jr.: 1989, *Astrophys. J.* **347**, 529.